Observation of a Resonance in $B^+ \to K^+\mu^+\mu^-$ Decays at Low Recoil

R. Aaij *et al.**
(LHCb Collaboration)

(Received 29 July 2013; revised manuscript received 20 August 2013; published 10 September 2013)

A broad peaking structure is observed in the dimuon spectrum of $B^+ \to K^+\mu^+\mu^-$ decays in the kinematic region where the kaon has a low recoil against the dimuon system. The structure is consistent with interference between the $B^+ \to K^+\mu^+\mu^-$ decay and a resonance and has a statistical significance exceeding six standard deviations. The mean and width of the resonance are measured to be 4191^{+9}_{-8} MeV/c^2 and 65^{+22}_{-16} MeV/c^2, respectively, where the uncertainties include statistical and systematic contributions. These measurements are compatible with the properties of the $\psi(4160)$ meson. First observations of both the decay $B^+ \to \psi(4160)K^+$ and the subsequent decay $\psi(4160) \to \mu^+\mu^-$ are reported. The resonant decay and the interference contribution make up 20% of the yield for dimuon masses above 3770 MeV/c^2. This contribution is larger than theoretical estimates.

DOI: 10.1103/PhysRevLett.111.112003 PACS numbers: 14.40.Pq, 13.20.He

The decay of the B^+ meson to the final state $K^+\mu^+\mu^-$ receives contributions from tree level decays and decays mediated through virtual quantum loop processes. The tree level decays proceed through the decay of a B^+ meson to a vector $c\bar{c}$ resonance and a K^+ meson, followed by the decay of the resonance to a pair of muons. Decays mediated by flavor changing neutral current (FCNC) loop processes give rise to pairs of muons with a nonresonant mass distribution. To probe contributions to the FCNC decay from physics beyond the standard model (SM), it is essential that the tree level decays are properly accounted for. In all analyses of the $B^+ \to K^+\mu^+\mu^-$ decay, from discovery [1] to the latest most accurate measurement [2], this has been done by placing a veto on the regions of dimuon mass $m_{\mu^+\mu^-}$ dominated by the J/ψ and $\psi(2S)$ resonances. In the low recoil region, corresponding to a dimuon mass above the open charm threshold, theoretical predictions of the decay rate can be obtained with an operator product expansion (OPE) [3] in which the $c\bar{c}$ contribution and other hadronic effects are treated as effective interactions.

Nearly all available information about the $J^{PC} = 1^{--}$ charmonium resonances above the open charm threshold, where the resonances are wide as decays to $D^{(*)}\bar{D}^{(*)}$ are allowed, comes from measurements of the cross-section ratio of $e^+e^- \to$ hadrons relative to $e^+e^- \to \mu^+\mu^-$. Among these analyses, only that of the BES Collaboration in Ref. [4] takes interference and strong phase differences between the different resonances into account. The broad and overlapping nature of these resonances means that they cannot be excluded by vetoes on the dimuon mass in an efficient way, and a more sophisticated treatment is required.

This Letter describes a measurement of a broad peaking structure in the low recoil region of the $B^+ \to K^+\mu^+\mu^-$ decay, based on data corresponding to an integrated luminosity of 3 fb^{-1} taken with the LHCb detector at a center-of-mass energy of 7 TeV in 2011 and 8 TeV in 2012. Fits to the dimuon mass spectrum are performed, where one or several resonances are allowed to interfere with the nonresonant $B^+ \to K^+\mu^+\mu^-$ signal, and their parameters determined. The inclusion of charge conjugated processes is implied throughout this Letter.

The LHCb detector [5] is a single-arm forward spectrometer covering the pseudorapidity range $2 < \eta < 5$, designed for the study of particles containing b or c quarks. The detector includes a high-precision tracking system consisting of a silicon-strip vertex detector surrounding the pp interaction region, a large-area silicon-strip detector located upstream of a dipole magnet with a bending power of about 4 Tm, and three stations of silicon-strip detectors and straw drift tubes placed downstream. The combined tracking system provides a momentum measurement with relative uncertainty that varies from 0.4% at 5 GeV/c to 0.6% at 100 GeV/c, and impact parameter resolution of 20 μm for tracks with high transverse momentum. Charged hadrons are identified using two ring-imaging Cherenkov detectors. Muons are identified by a system composed of alternating layers of iron and multiwire proportional chambers. Simulated events used in this analysis are produced using the software described in Refs. [6–11].

Candidates are required to pass a two stage trigger system [12]. In the initial hardware stage, candidate events are selected with at least one muon with transverse momentum, $p_T > 1.48\,(1.76)$ GeV/c in 2011 (2012). In the subsequent software stage, at least one of the final state particles is required to have both $p_T > 1.0$ GeV/c and

*Full author list given at end of the article.

impact parameter larger than 100 μm with respect to all of the primary pp interaction vertices (PVs) in the event. Finally, a multivariate algorithm [13] is used for the identification of secondary vertices consistent with the decay of a b hadron with muons in the final state.

The selection of the $K^+\mu^+\mu^-$ final state is made in two steps. Candidates are required to pass an initial selection, which reduces the data sample to a manageable level, followed by a multivariate selection. The dominant background is of a combinatorial nature, where two correctly identified muons from different heavy flavor hadron decays are combined with a kaon from either of those decays. This category of background has no peaking structure in either the dimuon mass or the $K^+\mu^+\mu^-$ mass. The signal region is defined as $5240 < m_{K^+\mu^+\mu^-} < 5320$ MeV/c^2 and the sideband region as $5350 < m_{K^+\mu^+\mu^-} < 5500$ MeV/c^2. The sideband below the B^+ mass is not used as it contains backgrounds from partially reconstructed decays, which do not contaminate the signal region.

The initial selection requires $\chi^2_{\rm IP} > 9$ for all final state particles, where $\chi^2_{\rm IP}$ is defined as the minimum change in χ^2 when the particle is included in a vertex fit to any of the PVs in the event, that the muons are positively identified in the muon system, and that the dimuon vertex has a vertex fit $\chi^2 < 9$. In addition, based on the lowest $\chi^2_{\rm IP}$ of the B^+ candidate, an associated PV is chosen. For this PV it is required that the B^+ candidate has $\chi^2_{\rm IP} < 16$, the vertex fit χ^2 must increase by more than 121 when including the B^+ candidate daughters, and the angle between the B^+ candidate momentum and the direction from the PV to the decay vertex should be below 14 mrad. Finally, the B^+ candidate is required to have a vertex fit $\chi^2 < 24$ (with 3 degrees of freedom).

The multivariate selection is based on a boosted decision tree (BDT) [14] with the AdaBoost algorithm [15] to separate signal from background. It is trained with a signal sample from simulation and a background sample consisting of 10% of the data from the sideband region. The multivariate selection uses geometric and kinematic variables, where the most discriminating variables are the $\chi^2_{\rm IP}$ of the final state particles and the vertex quality of the B^+ candidate. The selection with the BDT has an efficiency of 90% on signal surviving the initial selection while retaining 6% of the background. The overall efficiency for the reconstruction, trigger and selection, normalized to the total number of $B^+ \to K^+\mu^+\mu^-$ decays produced at the LHCb interaction point, is 2%. As the branching fraction measurements are normalized to the $B^+ \to J/\psi K^+$ decay, only relative efficiencies are used. The yields in the $K^+\mu^+\mu^-$ final state from $B^+ \to J/\psi K^+$ and $B^+ \to \psi(2S)K^+$ decays are 9.6×10^5 and 8×10^4 events, respectively.

In addition to the combinatorial background, there are several small sources of potential background that form a peak in either or both of the $m_{K^+\mu^+\mu^-}$ and $m_{\mu^+\mu^-}$ distributions. The largest of these backgrounds are the decays $B^+ \to J/\psi K^+$ and $B^+ \to \psi(2S)K^+$, where the kaon and one of the muons have been interchanged. The decays $B^+ \to K^+\pi^-\pi^+$ and $B^+ \to \bar{D}^0\pi^+$ followed by $\bar{D}^0 \to K^+\pi^-$, with the two pions identified as muons are also considered. To reduce these backgrounds to a negligible level, tight particle identification criteria and vetoes on μ^-K^+ combinations compatible with J/ψ, $\psi(2S)$, or D^0 meson decays are applied. These vetoes are 99% efficient on signal.

A kinematic fit [16] is performed for all selected candidates. In the fit the $K^+\mu^+\mu^-$ mass is constrained to the nominal B^+ mass and the candidate is required to originate from its associated PV. For $B^+ \to \psi(2S)K^+$ decays, this improves the resolution in $m_{\mu^+\mu^-}$ from 15 to 5 MeV/c^2. Given the widths of the resonances that are subsequently analyzed, resolution effects are neglected. While the $\psi(2S)$ state is narrow, the large branching fraction means that its non-Gaussian tail is significant and hard to model. The $\psi(2S)$ contamination is reduced to a negligible level by requiring $m_{\mu^+\mu^-} > 3770$ MeV/c^2. This dimuon mass range is defined as the low recoil region used in this analysis.

In order to estimate the amount of background present in the $m_{\mu^+\mu^-}$ spectrum, an unbinned extended maximum likelihood fit is performed to the $K^+\mu^+\mu^-$ mass distribution without the B^+ mass constraint. The signal shape is taken from a mass fit to the $B^+ \to \psi(2S)K^+$ mode in data with the shape parameterized as the sum of two Crystal Ball functions [17], with common tail parameters, but different widths. The Gaussian width of the two components is increased by 5% for the fit to the low recoil region as determined from simulation. The low recoil region contains 1830 candidates in the signal mass window, with a signal to background ratio of 7.8.

The dimuon mass distribution in the low recoil region is shown in Fig. 1. Two peaks are visible, one at the low edge corresponding to the expected decay $\psi(3770) \to \mu^+\mu^-$ and a wide peak at a higher mass. In all fits, a vector resonance component corresponding to this decay is

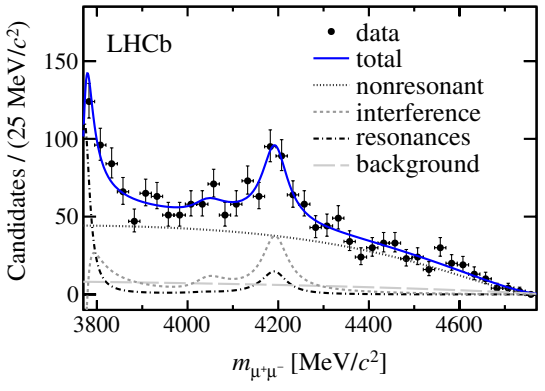

FIG. 1 (color online). Dimuon mass distribution of data with fit results overlaid for the fit that includes contributions from the nonresonant vector and axial vector components, and the $\psi(3770)$, $\psi(4040)$, and $\psi(4160)$ resonances. Interference terms are included and the relative strong phases are left free in the fit.

included. Several fits are made to the distribution. The first introduces a vector resonance with unknown parameters. Subsequent fits look at the compatibility of the data with the hypothesis that the peaking structure is due to known resonances.

The nonresonant part of the mass fits contains a vector and axial vector component. Of these, only the vector component will interfere with the resonance. The probability density function (PDF) of the signal component is given as

$$\mathcal{P}_{\rm sig} \propto P(m_{\mu^+\mu^-})|\mathcal{A}|^2 f^2(m^2_{\mu^+\mu^-}), \quad (1)$$

$$|\mathcal{A}|^2 = |A^{\rm V}_{\rm nr} + \sum_k e^{i\delta_k} A^k_{\rm r}|^2 + |A^{\rm AV}_{\rm nr}|^2, \quad (2)$$

where $A^{\rm V}_{\rm nr}$ and $A^{\rm AV}_{\rm nr}$ are the vector and axial vector amplitudes of the nonresonant decay. The shape of the nonresonant signal in $m_{\mu^+\mu^-}$ is driven by phase space, $P(m_{\mu^+\mu^-})$, and the form factor, $f(m^2_{\mu^+\mu^-})$. The parametrization of Ref. [18] is used to describe the dimuon mass dependence of the form factor. This form factor parametrization is consistent with recent lattice calculations [19]. In the SM at low recoil, the ratio of the vector and axial vector contributions to the nonresonant component is expected to have negligible dependence on the dimuon mass. The vector component accounts for $(45 \pm 6)\%$ of the differential branching fraction in the SM (see, for example, Ref. [20]). This estimate of the vector component is assumed in the fit.

The total vector amplitude is formed by summing the vector amplitude of the nonresonant signal with a number of Breit-Wigner amplitudes $A^k_{\rm r}$ which depend on $m_{\mu^+\mu^-}$. Each Breit-Wigner amplitude is rotated by a phase δ_k which represents the strong phase difference between the nonresonant vector component and the resonance with index k. Such phase differences are expected [18]. The $\psi(3770)$ resonance, visible at the lower edge of the dimuon mass distribution, is included in the fit as a Breit-Wigner component whose mass and width are constrained to the world average values [21].

The background PDF for the dimuon mass distribution is taken from a fit to data in the $K^+\mu^+\mu^-$ sideband. The uncertainties on the background amount and shape are included as Gaussian constraints to the fit in the signal region.

The signal PDF is multiplied by the relative efficiency as a function of dimuon mass with respect to the $B^+ \to J/\psi K^+$ decay. As in previous analyses of the same final state [22], this efficiency is determined from simulation after the simulation is made to match data by degrading by $\sim$20% the impact parameter resolution of the tracks, reweighting events to match the kinematic properties of the B^+ candidates and the track multiplicity of the event, and adjusting the particle identification variables based on calibration samples from data. In the region from the J/ψ mass to 4600 MeV/c^2 the relative efficiency drops by around 20%. From there to the kinematic end point it drops sharply, predominantly due to the $\chi^2_{\rm IP}$ cut on the kaon as in this region its direction is aligned with the B^+ candidate and therefore also with the PV.

Initially, a fit with a single resonance in addition to the $\psi(3770)$ and nonresonant terms is performed. This additional resonance has its phase, mean, and width left free. The parameters of the resonance returned by the fit are a mass of 4191^{+9}_{-8} MeV/c^2 and a width of 65^{+22}_{-16} MeV/c^2. Branching fractions are determined by integrating the square of the Breit-Wigner amplitude returned by the fit, normalizing to the $B^+ \to J/\psi K^+$ yield, and multiplying with the product of branching fractions, $\mathcal{B}(B^+ \to J/\psi K^+) \times \mathcal{B}(J/\psi \to \mu^+\mu^-)$ [21]. The product $\mathcal{B}(B^+ \to XK^+) \times \mathcal{B}(X \to \mu^+\mu^-)$ for the additional resonance X is determined to be $(3.9^{+0.7}_{-0.6}) \times 10^{-9}$. The uncertainty on this product is calculated using the profile likelihood. The data are not sensitive to the vector fraction of the nonresonant component as the branching fraction of the resonance will vary to compensate. For example, if the vector fraction is lowered to 30%, the central value of the branching fraction increases to 4.6×10^{-9}. This reflects the lower amount of interference allowed between the resonant and nonresonant components.

The significance of the resonance is obtained by simulating pseudoexperiments that include the nonresonant, $\psi(3770)$, and background components. The log likelihood ratios between fits that include and exclude a resonant component for 6×10^5 such samples are compared to the difference observed in fits to the data. None of the samples have a higher ratio than observed in data and an extrapolation gives a significance of the signal above 6 standard deviations.

The properties of the resonance are compatible with the mass and width of the $\psi(4160)$ resonance as measured in Ref. [4]. To test the hypothesis that ψ resonances well above the open charm threshold are observed, another fit including the $\psi(4040)$ and $\psi(4160)$ resonances is performed. The mass and width of the two are constrained to the measurements from Ref. [4]. The data have no sensitivity to a $\psi(4415)$ contribution. The fit describes the data well and the parameters of the $\psi(4160)$ meson are almost unchanged with respect to the unconstrained fit. The fit overlaid on the data is shown in Fig. 1 and Table I reports the fit parameters.

TABLE I. Parameters of the dominant resonance for fits where the mass and width are unconstrained and constrained to those of the $\psi(4160)$ meson [4], respectively. The branching fractions are for the B^+ decay followed by the decay of the resonance to muons.

	Unconstrained	$\psi(4160)$
$\mathcal{B}[\times 10^{-9}]$	$3.9^{+0.7}_{-0.6}$	$3.5^{+0.9}_{-0.8}$
Mass [MeV/c^2]	4191^{+9}_{-8}	4190 ± 5
Width [MeV/c^2]	65^{+22}_{-16}	66 ± 12
Phase [rad]	-1.7 ± 0.3	-1.8 ± 0.3

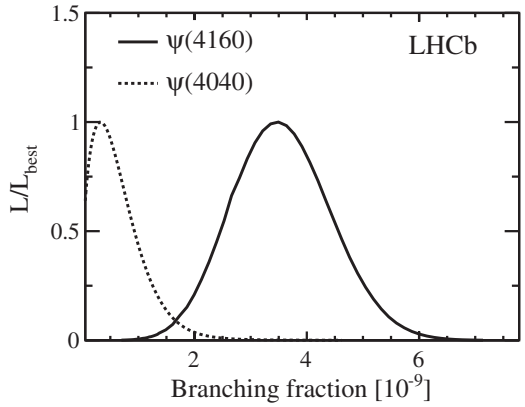

FIG. 2. Profile likelihood ratios for the product of branching fractions $\mathcal{B}(B^+ \to \psi K^+) \times \mathcal{B}(\psi \to \mu^+\mu^-)$ of the $\psi(4040)$ and the $\psi(4160)$ mesons. At each point all other fit parameters are reoptimized.

The resulting profile likelihood ratio compared to the best fit as a function of branching fraction can be seen in Fig. 2. In the fit with the three ψ resonances, the $\psi(4160)$ meson is visible with $\mathcal{B}(B^+ \to \psi(4160)K^+) \times \mathcal{B}(\psi(4160) \to \mu^+\mu^-) = (3.5^{+0.9}_{-0.8}) \times 10^{-9}$ but for the $\psi(4040)$ meson, no significant signal is seen, and an upper limit is set. The limit $\mathcal{B}(B^+ \to \psi(4040)K^+) \times \mathcal{B}(\psi(4040) \to \mu^+\mu^-) < 1.3\,(1.5) \times 10^{-9}$ at 90 (95)% confidence level is obtained by integrating the likelihood ratio compared to the best fit and assuming a flat prior for any positive branching fraction.

In Fig. 3 the likelihood scan of the fit with a single extra resonance is shown as a function of the mass and width of the resonance. The fit is compatible with the $\psi(4160)$ resonance, while a hypothesis where the resonance corresponds to the decay $Y(4260) \to \mu^+\mu^-$ is disfavored by more than 4 standard deviations.

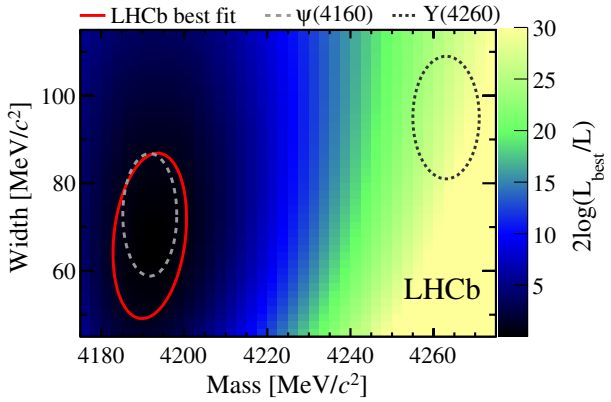

FIG. 3 (color online). Profile likelihood as a function of mass and width of a fit with a single extra resonance. At each point all other fit parameters are reoptimized. The three ellipses are (red, solid line) the best fit and previous measurements of (gray, dashed line) the $\psi(4160)$ [4] and (black, dotted line) the $Y(4260)$ [21] states.

Systematic uncertainties associated with the normalization procedure are negligible as the decay $B^+ \to J/\psi K^+$ has the same final state as the signal and similar kinematics. Uncertainties due to the resolution and mass scale are insignificant. The systematic uncertainty associated to the form factor parametrization in the fit model is taken from Ref. [20]. Finally, the uncertainty on the vector fraction of the nonresonant amplitude is obtained using the EOS tool described in Ref. [20] and is dominated by the uncertainty from short distance contributions. All systematic uncertainties are included in the fit as Gaussian constraints. From comparing the difference in the uncertainties on masses, widths and branching fractions for fits with and without these systematic constraints, it can be seen that the systematic uncertainties are about 20% the size of the statistical uncertainties and thus contribute less than 2% to the total uncertainty.

In summary, a resonance has been observed in the dimuon spectrum of $B^+ \to K^+\mu^+\mu^-$ decays with a significance of above 6 standard deviations. The resonance can be explained by the contribution of the $\psi(4160)$, via the decays $B^+ \to \psi(4160)K^+$ and $\psi(4160) \to \mu^+\mu^-$. It constitutes first observations of both decays. The $\psi(4160)$ is known to decay to electrons with a branching fraction of $(6.9 \pm 4.0) \times 10^{-6}$ [4]. Assuming lepton universality, the branching fraction of the decay $B^+ \to \psi(4160)K^+$ is measured to be $(5.1^{+1.3}_{-1.2} \pm 3.0) \times 10^{-4}$, where the second uncertainty corresponds to the uncertainty on the $\psi(4160) \to e^+e^-$ branching fraction. The corresponding limit for $B^+ \to \psi(4040)K^+$ is calculated to be $1.3\,(1.7) \times 10^{-4}$ at a 90 (95)% confidence level. The absence of the decay $B^+ \to \psi(4040)K^+$ at a similar level is interesting, and suggests future studies of $B^+ \to K^+\mu^+\mu^-$ decays based on larger data sets may reveal new insights into $c\bar{c}$ spectroscopy.

The contribution of the $\psi(4160)$ resonance in the low recoil region, taking into account interference with the nonresonant $B^+ \to K^+\mu^+\mu^-$ decay, is about 20% of the total signal. This value is larger than theoretical estimates, where the $c\bar{c}$ contribution is $\sim$10% of the vector amplitude, with a small correction from quark-hadron duality violation [23]. Results presented in this Letter will play an important role in controlling charmonium effects in future inclusive and exclusive $b \to s\mu^+\mu^-$ measurements.

We express our gratitude to our colleagues in the CERN accelerator departments for the excellent performance of the LHC. We thank the technical and administrative staff at the LHCb institutes. We acknowledge support from CERN and from the following national agencies: CAPES, CNPq, FAPERJ and FINEP (Brazil); NSFC (China); CNRS/IN2P3 and Region Auvergne (France); BMBF, DFG, HGF and MPG (Germany); SFI (Ireland); INFN (Italy); FOM and NWO (The Netherlands); SCSR (Poland); MEN/IFA (Romania); MinES, Rosatom, RFBR and NRC "Kurchatov Institute" (Russia); MinECo, XuntaGal and

GENCAT (Spain); SNSF and SER (Switzerland); NAS Ukraine (Ukraine); STFC (United Kingdom); NSF (USA). We also acknowledge the support received from the ERC under FP7. The Tier1 computing centers are supported by IN2P3 (France), KIT and BMBF (Germany), INFN (Italy), NWO and SURF (Netherlands), PIC (Spain), GridPP (United Kingdom). We are thankful for the computing resources put at our disposal by Yandex LLC (Russia), as well as to the communities behind the multiple open source software packages that we depend on.

[1] K. Abe *et al.* (Belle Collaboration), Phys. Rev. Lett. **88**, 021801 (2001).
[2] R. Aaij *et al.* (LHCb Collaboration), J. High Energy Phys. 02 (2013) 105.
[3] B. Grinstein and D. Pirjol, Phys. Rev. D **70**, 114005 (2004).
[4] M. Ablikim *et al.* (BES Collaboration), Phys. Lett. B **660**, 315 (2008).
[5] A. A. Alves, Jr. *et al.* (LHCb Collaboration), JINST **3**, S08005 (2008).
[6] T. Sjöstrand, S. Mrenna, and P. Skands, J. High Energy Phys. 05 (2006) 026.
[7] I. Belyaev *et al.*, Nuclear Science Symposium Conference Record (NSS/MIC) IEEE, 1155 (2010).
[8] D. J. Lange, Nucl. Instrum. Methods Phys. Res., Sect. A **462**, 152 (2001).
[9] P. Golonka and Z. Was, Eur. Phys. J. C **45**, 97 (2006).
[10] J. Allison *et al.* (Geant4 Collaboration), IEEE Trans. Nucl. Sci. **53**, 270 (2006); S. Agostinelli *et al.* (Geant4 Collaboration), Nucl. Instrum. Methods Phys. Res., Sect. A **506**, 250 (2003).
[11] M. Clemencic, G. Corti, S. Easo, C. R. Jones, S. Miglioranzi, M. Pappagallo, and P. Robbe, J. Phys. Conf. Ser. **331**, 032023 (2011).
[12] R. Aaij *et al.*, JINST **8**, P04022 (2013).
[13] V. V. Gligorov and M. Williams, JINST **8**, P02013 (2013).
[14] L. Breiman, J. H. Friedman, R. A. Olshen, and C. J. Stone, *Classification and Regression Trees* (Wadsworth International Group, Belmont, California, 1984).
[15] R. E. Schapire and Y. Freund, J. Comput. Syst. Sci. **55**, 119 (1997).
[16] W. D. Hulsbergen, Nucl. Instrum. Methods Phys. Res., Sect. A **552**, 566 (2005).
[17] T. Skwarnicki, Ph.D. thesis, Institute of Nuclear Physics, Krakow, 1986.
[18] A. Khodjamirian, Th. Mannel, A. A. Pivovarov, and Y.-M. Wang, J. High Energy Phys. 09 (2010) 089.
[19] C. Bouchard *et al.*, arXiv:1306.2384.
[20] C. Bobeth, G. Hiller, D. van Dyk, and C. Wacker, J. High Energy Phys. 01 (2012) 107.
[21] J. Beringer *et al.* (Particle Data Group), Phys. Rev. D **86**, 010001 (2012).
[22] R. Aaij *et al.* (LHCb Collaboration), J. High Energy Phys. 07 (2012) 133.
[23] M. Beylich, G. Buchalla, and T. Feldmann, Eur. Phys. J. C **71**, 1635 (2011).

R. Aaij,[40] B. Adeva,[36] M. Adinolfi,[45] C. Adrover,[6] A. Affolder,[51] Z. Ajaltouni,[5] J. Albrecht,[9] F. Alessio,[37] M. Alexander,[50] S. Ali,[40] G. Alkhazov,[29] P. Alvarez Cartelle,[36] A. A. Alves, Jr.,[24,37] S. Amato,[2] S. Amerio,[21] Y. Amhis,[7] L. Anderlini,[17,f] J. Anderson,[39] R. Andreassen,[56] J. E. Andrews,[57] R. B. Appleby,[53] O. Aquines Gutierrez,[10] F. Archilli,[18] A. Artamonov,[34] M. Artuso,[58] E. Aslanides,[6] G. Auriemma,[24,m] M. Baalouch,[5] S. Bachmann,[11] J. J. Back,[47] C. Baesso,[59] V. Balagura,[30] W. Baldini,[16] R. J. Barlow,[53] C. Barschel,[37] S. Barsuk,[7] W. Barter,[46] Th. Bauer,[40] A. Bay,[38] J. Beddow,[50] F. Bedeschi,[22] I. Bediaga,[1] S. Belogurov,[30] K. Belous,[34] I. Belyaev,[30] E. Ben-Haim,[8] G. Bencivenni,[18] S. Benson,[49] J. Benton,[45] A. Berezhnoy,[31] R. Bernet,[39] M.-O. Bettler,[46] M. van Beuzekom,[40] A. Bien,[11] S. Bifani,[44] T. Bird,[53] A. Bizzeti,[17,h] P. M. Bjørnstad,[53] T. Blake,[37] F. Blanc,[38] J. Blouw,[11] S. Blusk,[58] V. Bocci,[24] A. Bondar,[33] N. Bondar,[29] W. Bonivento,[15] S. Borghi,[53] A. Borgia,[58] T. J. V. Bowcock,[51] E. Bowen,[39] C. Bozzi,[16] T. Brambach,[9] J. van den Brand,[41] J. Bressieux,[38] D. Brett,[53] M. Britsch,[10] T. Britton,[58] N. H. Brook,[45] H. Brown,[51] I. Burducea,[28] A. Bursche,[39] G. Busetto,[21,q] J. Buytaert,[37] S. Cadeddu,[15] O. Callot,[7] M. Calvi,[20,j] M. Calvo Gomez,[35,n] A. Camboni,[35] P. Campana,[18,37] D. Campora Perez,[37] A. Carbone,[14,c] G. Carboni,[23,k] R. Cardinale,[19,i] A. Cardini,[15] H. Carranza-Mejia,[49] L. Carson,[52] K. Carvalho Akiba,[2] G. Casse,[51] L. Castillo Garcia,[37] M. Cattaneo,[37] Ch. Cauet,[9] R. Cenci,[57] M. Charles,[54] Ph. Charpentier,[37] P. Chen,[3,38] N. Chiapolini,[39] M. Chrzaszcz,[25] K. Ciba,[37] X. Cid Vidal,[37] G. Ciezarek,[52] P. E. L. Clarke,[49] M. Clemencic,[37] H. V. Cliff,[46] J. Closier,[37] C. Coca,[28] V. Coco,[40] J. Cogan,[6] E. Cogneras,[5] P. Collins,[37] A. Comerma-Montells,[35] A. Contu,[15,37] A. Cook,[45] M. Coombes,[45] S. Coquereau,[8] G. Corti,[37] B. Couturier,[37] G. A. Cowan,[49] E. Cowie,[45] D. C. Craik,[47] S. Cunliffe,[52] R. Currie,[49] C. D'Ambrosio,[37] P. David,[8] P. N. Y. David,[40] A. Davis,[56] I. De Bonis,[4] K. De Bruyn,[40] S. De Capua,[53] M. De Cian,[11] J. M. De Miranda,[1] L. De Paula,[2] W. De Silva,[56] P. De Simone,[18] D. Decamp,[4] M. Deckenhoff,[9] L. Del Buono,[8] N. Déléage,[4] D. Derkach,[54] O. Deschamps,[5] F. Dettori,[41] A. Di Canto,[11] H. Dijkstra,[37] M. Dogaru,[28] S. Donleavy,[51] F. Dordei,[11] A. Dosil Suárez,[36] D. Dossett,[47] A. Dovbnya,[42] F. Dupertuis,[38] P. Durante,[37] R. Dzhelyadin,[34] A. Dziurda,[25] A. Dzyuba,[29] S. Easo,[48] U. Egede,[52] V. Egorychev,[30] S. Eidelman,[33] D. van Eijk,[40] S. Eisenhardt,[49] U. Eitschberger,[9] R. Ekelhof,[9] L. Eklund,[50,37]

I. El Rifai,[5] Ch. Elsasser,[39] A. Falabella,[14,e] C. Färber,[11] G. Fardell,[49] C. Farinelli,[40] S. Farry,[51] D. Ferguson,[49] V. Fernandez Albor,[36] F. Ferreira Rodrigues,[1] M. Ferro-Luzzi,[37] S. Filippov,[32] M. Fiore,[16] C. Fitzpatrick,[37] M. Fontana,[10] F. Fontanelli,[19,i] R. Forty,[37] O. Francisco,[2] M. Frank,[37] C. Frei,[37] M. Frosini,[17,f] S. Furcas,[20] E. Furfaro,[23,k] A. Gallas Torreira,[36] D. Galli,[14,c] M. Gandelman,[2] P. Gandini,[58] Y. Gao,[3] J. Garofoli,[58] P. Garosi,[53] J. Garra Tico,[46] L. Garrido,[35] C. Gaspar,[37] R. Gauld,[54] E. Gersabeck,[11] M. Gersabeck,[53] T. Gershon,[47,37] Ph. Ghez,[4] V. Gibson,[46] L. Giubega,[28] V. V. Gligorov,[37] C. Göbel,[59] D. Golubkov,[30] A. Golutvin,[52,30,37] A. Gomes,[2] P. Gorbounov,[30,37] H. Gordon,[37] C. Gotti,[20] M. Grabalosa Gándara,[5] R. Graciani Diaz,[35] L. A. Granado Cardoso,[37] E. Graugés,[35] G. Graziani,[17] A. Grecu,[28] E. Greening,[54] S. Gregson,[46] P. Griffith,[44] O. Grünberg,[60] B. Gui,[58] E. Gushchin,[32] Yu. Guz,[34,37] T. Gys,[37] C. Hadjivasiliou,[58] G. Haefeli,[38] C. Haen,[37] S. C. Haines,[46] S. Hall,[52] B. Hamilton,[57] T. Hampson,[45] S. Hansmann-Menzemer,[11] N. Harnew,[54] S. T. Harnew,[45] J. Harrison,[53] T. Hartmann,[60] J. He,[37] T. Head,[37] V. Heijne,[40] K. Hennessy,[51] P. Henrard,[5] J. A. Hernando Morata,[36] E. van Herwijnen,[37] M. Hess,[60] A. Hicheur,[1] E. Hicks,[51] D. Hill,[54] M. Hoballah,[5] C. Hombach,[53] P. Hopchev,[4] W. Hulsbergen,[40] P. Hunt,[54] T. Huse,[51] N. Hussain,[54] D. Hutchcroft,[51] D. Hynds,[50] V. Iakovenko,[43] M. Idzik,[26] P. Ilten,[12] R. Jacobsson,[37] A. Jaeger,[11] E. Jans,[40] P. Jaton,[38] A. Jawahery,[57] F. Jing,[3] M. John,[54] D. Johnson,[54] C. R. Jones,[46] C. Joram,[37] B. Jost,[37] M. Kaballo,[9] S. Kandybei,[42] W. Kanso,[6] M. Karacson,[37] T. M. Karbach,[37] I. R. Kenyon,[44] T. Ketel,[41] A. Keune,[38] B. Khanji,[20] O. Kochebina,[7] I. Komarov,[38] R. F. Koopman,[41] P. Koppenburg,[40] M. Korolev,[31] A. Kozlinskiy,[40] L. Kravchuk,[32] K. Kreplin,[11] M. Kreps,[47] G. Krocker,[11] P. Krokovny,[33] F. Kruse,[9] M. Kucharczyk,[20,25,j] V. Kudryavtsev,[33] K. Kurek,[27] T. Kvaratskheliya,[30,37] V. N. La Thi,[38] D. Lacarrere,[37] G. Lafferty,[53] A. Lai,[15] D. Lambert,[49] R. W. Lambert,[41] E. Lanciotti,[37] G. Lanfranchi,[18] C. Langenbruch,[37] T. Latham,[47] C. Lazzeroni,[44] R. Le Gac,[6] J. van Leerdam,[40] J.-P. Lees,[4] R. Lefèvre,[5] A. Leflat,[31] J. Lefrançois,[7] S. Leo,[22] O. Leroy,[6] T. Lesiak,[25] B. Leverington,[11] Y. Li,[3] L. Li Gioi,[5] M. Liles,[51] R. Lindner,[37] C. Linn,[11] B. Liu,[3] G. Liu,[37] S. Lohn,[37] I. Longstaff,[50] J. H. Lopes,[2] N. Lopez-March,[38] H. Lu,[3] D. Lucchesi,[21,q] J. Luisier,[38] H. Luo,[49] F. Machefert,[7] I. V. Machikhiliyan,[4,30] F. Maciuc,[28] O. Maev,[29,37] S. Malde,[54] G. Manca,[15,d] G. Mancinelli,[6] J. Maratas,[5] U. Marconi,[14] P. Marino,[22,s] R. Märki,[38] J. Marks,[11] G. Martellotti,[24] A. Martens,[8] A. Martín Sánchez,[7] M. Martinelli,[40] D. Martinez Santos,[41] D. Martins Tostes,[2] A. Martynov,[31] A. Massafferri,[1] R. Matev,[37] Z. Mathe,[37] C. Matteuzzi,[20] E. Maurice,[6] A. Mazurov,[16,32,37,e] J. McCarthy,[44] A. McNab,[53] R. McNulty,[12] B. McSkelly,[51] B. Meadows,[56,54] F. Meier,[9] M. Meissner,[11] M. Merk,[40] D. A. Milanes,[8] M.-N. Minard,[4] J. Molina Rodriguez,[59] S. Monteil,[5] D. Moran,[53] P. Morawski,[25] A. Mordà,[6] M. J. Morello,[22,s] R. Mountain,[58] I. Mous,[40] F. Muheim,[49] K. Müller,[39] R. Muresan,[28] B. Muryn,[26] B. Muster,[38] P. Naik,[45] T. Nakada,[38] R. Nandakumar,[48] I. Nasteva,[1] M. Needham,[49] S. Neubert,[37] N. Neufeld,[37] A. D. Nguyen,[38] T. D. Nguyen,[38] C. Nguyen-Mau,[38,o] M. Nicol,[7] V. Niess,[5] R. Niet,[9] N. Nikitin,[31] T. Nikodem,[11] A. Nomerotski,[54] A. Novoselov,[34] A. Oblakowska-Mucha,[26] V. Obraztsov,[34] S. Oggero,[40] S. Ogilvy,[50] O. Okhrimenko,[43] R. Oldeman,[15,d] M. Orlandea,[28] J. M. Otalora Goicochea,[2] P. Owen,[52] A. Oyanguren,[35] B. K. Pal,[58] A. Palano,[13,b] T. Palczewski,[27] M. Palutan,[18] J. Panman,[37] A. Papanestis,[48] M. Pappagallo,[50] C. Parkes,[53] C. J. Parkinson,[52] G. Passaleva,[17] G. D. Patel,[51] M. Patel,[52] G. N. Patrick,[48] C. Patrignani,[19,i] C. Pavel-Nicorescu,[28] A. Pazos Alvarez,[36] A. Pellegrino,[40] G. Penso,[24,l] M. Pepe Altarelli,[37] S. Perazzini,[14,c] E. Perez Trigo,[36] A. Pérez-Calero Yzquierdo,[35] P. Perret,[5] M. Perrin-Terrin,[6] L. Pescatore,[44] E. Pesen,[61] K. Petridis,[52] A. Petrolini,[19,i] A. Phan,[58] E. Picatoste Olloqui,[35] B. Pietrzyk,[4] T. Pilař,[47] D. Pinci,[24] S. Playfer,[49] M. Plo Casasus,[36] F. Polci,[8] G. Polok,[25] A. Poluektov,[47,33] E. Polycarpo,[2] A. Popov,[34] D. Popov,[10] B. Popovici,[28] C. Potterat,[35] A. Powell,[54] J. Prisciandaro,[38] A. Pritchard,[51] C. Prouve,[7] V. Pugatch,[43] A. Puig Navarro,[38] G. Punzi,[22,r] W. Qian,[4] J. H. Rademacker,[45] B. Rakotomiaramanana,[38] M. S. Rangel,[2] I. Raniuk,[42] N. Rauschmayr,[37] G. Raven,[41] S. Redford,[54] M. M. Reid,[47] A. C. dos Reis,[1] S. Ricciardi,[48] A. Richards,[52] K. Rinnert,[51] V. Rives Molina,[35] D. A. Roa Romero,[5] P. Robbe,[7] D. A. Roberts,[57] E. Rodrigues,[53] P. Rodriguez Perez,[36] S. Roiser,[37] V. Romanovsky,[34] A. Romero Vidal,[36] J. Rouvinet,[38] T. Ruf,[37] F. Ruffini,[22] H. Ruiz,[35] P. Ruiz Valls,[35] G. Sabatino,[24,k] J. J. Saborido Silva,[36] N. Sagidova,[29] P. Sail,[50] B. Saitta,[15,d] V. Salustino Guimaraes,[2] B. Sanmartin Sedes,[36] M. Sannino,[19,i] R. Santacesaria,[24] C. Santamarina Rios,[36] E. Santovetti,[23,k] M. Sapunov,[6] A. Sarti,[18,l] C. Satriano,[24,m] A. Satta,[23] M. Savrie,[16,e] D. Savrina,[30,31] P. Schaack,[52] M. Schiller,[41] H. Schindler,[37] M. Schlupp,[9] M. Schmelling,[10] B. Schmidt,[37] O. Schneider,[38] A. Schopper,[37] M.-H. Schune,[7] R. Schwemmer,[37] B. Sciascia,[18] A. Sciubba,[24] M. Seco,[36] A. Semennikov,[30] K. Senderowska,[26] I. Sepp,[52] N. Serra,[39] J. Serrano,[6] P. Seyfert,[11] M. Shapkin,[34] I. Shapoval,[16,42] P. Shatalov,[30] Y. Shcheglov,[29] T. Shears,[51,37] L. Shekhtman,[33] O. Shevchenko,[42] V. Shevchenko,[30] A. Shires,[9] R. Silva Coutinho,[47] M. Sirendi,[46] N. Skidmore,[45] T. Skwarnicki,[58]

N. A. Smith,[51] E. Smith,[54,48] J. Smith,[46] M. Smith,[53] M. D. Sokoloff,[56] F. J. P. Soler,[50] F. Soomro,[38] D. Souza,[45] B. Souza De Paula,[2] B. Spaan,[9] A. Sparkes,[49] P. Spradlin,[50] F. Stagni,[37] S. Stahl,[11] O. Steinkamp,[39] S. Stevenson,[54] S. Stoica,[28] S. Stone,[58] B. Storaci,[39] M. Straticiuc,[28] U. Straumann,[39] V. K. Subbiah,[37] L. Sun,[56] S. Swientek,[9] V. Syropoulos,[41] M. Szczekowski,[27] P. Szczypka,[38,37] T. Szumlak,[26] S. T'Jampens,[4] M. Teklishyn,[7] E. Teodorescu,[28] F. Teubert,[37] C. Thomas,[54] E. Thomas,[37] J. van Tilburg,[11] V. Tisserand,[4] M. Tobin,[38] S. Tolk,[41] D. Tonelli,[37] S. Topp-Joergensen,[54] N. Torr,[54] E. Tournefier,[4,52] S. Tourneur,[38] M. T. Tran,[38] M. Tresch,[39] A. Tsaregorodtsev,[6] P. Tsopelas,[40] N. Tuning,[40] M. Ubeda Garcia,[37] A. Ukleja,[27] D. Urner,[53] A. Ustyuzhanin,[52,p] U. Uwer,[11] V. Vagnoni,[14] G. Valenti,[14] A. Vallier,[7] M. Van Dijk,[45] R. Vazquez Gomez,[18] P. Vazquez Regueiro,[36] C. Vázquez Sierra,[36] S. Vecchi,[16] J. J. Velthuis,[45] M. Veltri,[17,g] G. Veneziano,[38] M. Vesterinen,[37] B. Viaud,[7] D. Vieira,[2] X. Vilasis-Cardona,[35,n] A. Vollhardt,[39] D. Volyanskyy,[10] D. Voong,[45] A. Vorobyev,[29] V. Vorobyev,[33] C. Voß,[60] H. Voss,[10] R. Waldi,[60] C. Wallace,[47] R. Wallace,[12] S. Wandernoth,[11] J. Wang,[58] D. R. Ward,[46] N. K. Watson,[44] A. D. Webber,[53] D. Websdale,[52] M. Whitehead,[47] J. Wicht,[37] J. Wiechczynski,[25] D. Wiedner,[11] L. Wiggers,[40] G. Wilkinson,[54] M. P. Williams,[47,48] M. Williams,[55] F. F. Wilson,[48] J. Wimberley,[57] J. Wishahi,[9] W. Wislicki,[27] M. Witek,[25] S. A. Wotton,[46] S. Wright,[46] S. Wu,[3] K. Wyllie,[37] Y. Xie,[49,37] Z. Xing,[58] Z. Yang,[3] R. Young,[49] X. Yuan,[3] O. Yushchenko,[34] M. Zangoli,[14] M. Zavertyaev,[10,a] F. Zhang,[3] L. Zhang,[58] W. C. Zhang,[12] Y. Zhang,[3] A. Zhelezov,[11] A. Zhokhov,[30] L. Zhong,[3] and A. Zvyagin[37]

(LHCb Collaboration)

[1]*Centro Brasileiro de Pesquisas Físicas (CBPF), Rio de Janeiro, Brazil*
[2]*Universidade Federal do Rio de Janeiro (UFRJ), Rio de Janeiro, Brazil*
[3]*Center for High Energy Physics, Tsinghua University, Beijing, China*
[4]*LAPP, Université de Savoie, CNRS/IN2P3, Annecy-Le-Vieux, France*
[5]*Clermont Université, Université Blaise Pascal, CNRS/IN2P3, LPC, Clermont-Ferrand, France*
[6]*CPPM, Aix-Marseille Université, CNRS/IN2P3, Marseille, France*
[7]*LAL, Université Paris-Sud, CNRS/IN2P3, Orsay, France*
[8]*LPNHE, Université Pierre et Marie Curie, Université Paris Diderot, CNRS/IN2P3, Paris, France*
[9]*Fakultät Physik, Technische Universität Dortmund, Dortmund, Germany*
[10]*Max-Planck-Institut für Kernphysik (MPIK), Heidelberg, Germany*
[11]*Physikalisches Institut, Ruprecht-Karls-Universität Heidelberg, Heidelberg, Germany*
[12]*School of Physics, University College Dublin, Dublin, Ireland*
[13]*Sezione INFN di Bari, Bari, Italy*
[14]*Sezione INFN di Bologna, Bologna, Italy*
[15]*Sezione INFN di Cagliari, Cagliari, Italy*
[16]*Sezione INFN di Ferrara, Ferrara, Italy*
[17]*Sezione INFN di Firenze, Firenze, Italy*
[18]*Laboratori Nazionali dell'INFN di Frascati, Frascati, Italy*
[19]*Sezione INFN di Genova, Genova, Italy*
[20]*Sezione INFN di Milano Bicocca, Milano, Italy*
[21]*Sezione INFN di Padova, Padova, Italy*
[22]*Sezione INFN di Pisa, Pisa, Italy*
[23]*Sezione INFN di Roma Tor Vergata, Roma, Italy*
[24]*Sezione INFN di Roma La Sapienza, Roma, Italy*
[25]*Henryk Niewodniczanski Institute of Nuclear Physics Polish Academy of Sciences, Kraków, Poland*
[26]*Faculty of Physics and Applied Computer Science, AGH-University of Science and Technology, Kraków, Poland*
[27]*National Center for Nuclear Research (NCBJ), Warsaw, Poland*
[28]*Horia Hulubei National Institute of Physics and Nuclear Engineering, Bucharest-Magurele, Romania*
[29]*Petersburg Nuclear Physics Institute (PNPI), Gatchina, Russia*
[30]*Institute of Theoretical and Experimental Physics (ITEP), Moscow, Russia*
[31]*Institute of Nuclear Physics, Moscow State University (SINP MSU), Moscow, Russia*
[32]*Institute for Nuclear Research of the Russian Academy of Sciences (INR RAN), Moscow, Russia*
[33]*Budker Institute of Nuclear Physics (SB RAS) and Novosibirsk State University, Novosibirsk, Russia*
[34]*Institute for High Energy Physics (IHEP), Protvino, Russia*
[35]*Universitat de Barcelona, Barcelona, Spain*
[36]*Universidad de Santiago de Compostela, Santiago de Compostela, Spain*
[37]*European Organization for Nuclear Research (CERN), Geneva, Switzerland*
[38]*Ecole Polytechnique Fédérale de Lausanne (EPFL), Lausanne, Switzerland*

[39]*Physik-Institut, Universität Zürich, Zürich, Switzerland*
[40]*Nikhef National Institute for Subatomic Physics, Amsterdam, The Netherlands*
[41]*Nikhef National Institute for Subatomic Physics and VU University Amsterdam, Amsterdam, The Netherlands*
[42]*NSC Kharkiv Institute of Physics and Technology (NSC KIPT), Kharkiv, Ukraine*
[43]*Institute for Nuclear Research of the National Academy of Sciences (KINR), Kyiv, Ukraine*
[44]*University of Birmingham, Birmingham, United Kingdom*
[45]*H.H. Wills Physics Laboratory, University of Bristol, Bristol, United Kingdom*
[46]*Cavendish Laboratory, University of Cambridge, Cambridge, United Kingdom*
[47]*Department of Physics, University of Warwick, Coventry, United Kingdom*
[48]*STFC Rutherford Appleton Laboratory, Didcot, United Kingdom*
[49]*School of Physics and Astronomy, University of Edinburgh, Edinburgh, United Kingdom*
[50]*School of Physics and Astronomy, University of Glasgow, Glasgow, United Kingdom*
[51]*Oliver Lodge Laboratory, University of Liverpool, Liverpool, United Kingdom*
[52]*Imperial College London, London, United Kingdom*
[53]*School of Physics and Astronomy, University of Manchester, Manchester, United Kingdom*
[54]*Department of Physics, University of Oxford, Oxford, United Kingdom*
[55]*Massachusetts Institute of Technology, Cambridge, Massachusetts, United States*
[56]*University of Cincinnati, Cincinnati, Ohio, United States*
[57]*University of Maryland, College Park, Maryland, United States*
[58]*Syracuse University, Syracuse, New York, United States*
[59]*Pontifícia Universidade Católica do Rio de Janeiro (PUC-Rio), Rio de Janeiro, Brazil, associated to Universidade Federal do Rio de Janeiro (UFRJ), Rio de Janeiro, Brazil*
[60]*Institut für Physik, Universität Rostock, Rostock, Germany, associated to Physikalisches Institut, Ruprecht-Karls-Universität Heidelberg, Heidelberg, Germany*
[61]*Celal Bayar University, Manisa, Turkey, associated to European Organization for Nuclear Research (CERN), Geneva, Switzerland*

[a]P.N. Lebedev Physical Institute, Russian Academy of Science (LPI RAS), Moscow, Russia.
[b]Università di Bari, Bari, Italy.
[c]Università di Bologna, Bologna, Italy.
[d]Università di Cagliari, Cagliari, Italy.
[e]Università di Ferrara, Ferrara, Italy.
[f]Università di Firenze, Firenze, Italy.
[g]Università di Urbino, Urbino, Italy.
[h]Università di Modena e Reggio Emilia, Modena, Italy.
[i]Università di Genova, Genova, Italy.
[j]Università di Milano Bicocca, Milano, Italy.
[k]Università di Roma Tor Vergata, Roma, Italy.
[l]Università di Roma La Sapienza, Roma, Italy.
[m]Università della Basilicata, Potenza, Italy.
[n]LIFAELS, La Salle, Universitat Ramon Llull, Barcelona, Spain.
[o]Hanoi University of Science, Hanoi, Viet Nam.
[p]Institute of Physics and Technology, Moscow, Russia.
[q]Università di Padova, Padova, Italy.
[r]Università di Pisa, Pisa, Italy.
[s]Scuola Normale Superiore, Pisa, Italy.